# The Quantitative Assessment of the Secreted IgG Repertoire after Recall to Evaluate the Quality of Immunizations

Klaus Eyer, Carlos Castrillon, Guilhem Chenon, Jérôme Bibette, Pierre Bruhns, Andrew D. Griffiths, Jean Baudry

# The Quantitative Assessment of the Secreted IgG Repertoire after Recall to Evaluate the Quality of Immunizations

**Klaus Eyer,*,† Carlos Castrillon,‡,§,¶ Guilhem Chenon,* Jérôme Bibette,* Pierre Bruhns,‡ Andrew D. Griffiths,§ and Jean Baudry***

**One of the major goals of vaccination is to prepare the body to rapidly secrete specific Abs during an infection. Assessment of the vaccine quality is often difficult to perform, as simple measurements like Ab titer only partly correlate with protection. Similarly, these simple measurements are not always sensitive to changes in the preceding immunization scheme. Therefore, we introduce in this paper a new, to our knowledge, method to assay the quality of immunization schemes for mice: shortly after a recall with pure Ag, we analyze the frequencies of IgG-secreting cells (IgG-SCs) in the spleen, as well as for each cells, the Ag affinity of the secreted Abs. We observed that after recall, appearance of the IgG-SCs within the spleen of immunized mice was fast (<24 h) and this early response was free of naive IgG-SCs. We further confirmed that our phenotypic analysis of IgG-SCs after recall strongly correlated with the different employed immunization schemes. Additionally, a phenotypic comparison of IgG-SCs presented in the spleen during immunization or after recall revealed similarities but also significant differences. The developed approach introduced a novel (to our knowledge), quantitative, and functional highly resolved alternative to study the quality of immunizations.** ***The Journal of Immunology*****, 2020, 205: 1176–1184.**

Exposure to an Ag through immunization often leads to the generation of an Ag-affine, functionally active and diverse Ab repertoire within the host organism (1–3). The processes to generate Ig G-secreting cells (IgG-SCs), often mediators of functionality and protection, are highly complex and involve different cellular pathways within and throughout the innate, adaptive, and humoral immune system (4–6). Additionally, the underlying processes shaping the IgG repertoire through generation, maturation, selection, and transfer are highly dynamic and changing over time (7–10), further complicating the problem. Because of this complexity, current characterizations after immunization are mainly centered on the final result (i.e., the secreted IgGs in the serum by measuring the Ab titer) (11, 12). Although simple and robust, titer measurements represent an average of the present IgG repertoire. Moreover, Ab titer only partly correlates with protection, even for Ab-mediated vaccines (13). Indeed, this measure is not suitable to resolve the full complexity of the humoral response in terms of biochemical ($>10^3$ different Abs in serum) (14), biophysical (affinity, specificity), or temporal dimensions (long half-lives, large distribution volume) (15, 16).

Because every IgG-SC was found to secrete only one variant of said isotype at a given time (17), an alternative approach would be the analysis of the humoral response on a cellular level. Such a measurement might serve as a good surrogate for the quality of the induced IgG repertoire, which is linked to the present diversity of Abs, in terms of affinity and specificity. This approach further allowed analyzing each secreted Ab separately, and to characterize each Ab as a "monoclonal" species. Applications using flow cytometry together with secretion inhibitors (18) and ELISPOT assay (19, 20) have been used to phenotypically characterize the present IgG repertoires. Although good to characterize frequencies of IgG-SCs, only a rough qualitative biochemical and biophysical description of the diversity and quality of the present IgG repertoire was achieved by applying these methods. Recently, next generation sequencing approaches with single-Ab resolution have been developed to probe the IgG repertoire more deeply (21–24). However, the coupling of these measures with a deep functional characterization of the IgG repertoire has been limited because of the need to re-express and characterize the Abs afterward, and no information about the functionality was gathered. To study the IgG repertoire's diversity and quality with resolution, we recently have described a technology that allowed a thorough ex vivo analysis of the secreted IgG repertoire called "DropMap" (Fig. 1) (8). This method allowed us to characterize the response with single-Ab resolution and to further extract functional information from each individually secreted IgG such as specificities, secretion rates (linked to concentration in the serum) and affinities (in this study expressed as dissociation constants, $K_D$). This allowed studying the secreted IgG repertoire with single-Ab; biochemical and physical resolution within the secreting cells. In our first study,

*Laboratoire Colloïdes et Matériaux Divisés, Institut Chimie, Biologie, Innovation, UMR8231, ESPCI Paris, CNRS, Université Paris Sciences et Lettres, 75005 Paris, France; †Laboratory for Functional Immune Repertoire Analysis, Institute of Pharmaceutical Sciences, Department of Chemistry and Applied Biology, ETH Zürich, 8093 Zurich, Switzerland; ‡Unit of Antibodies in Therapy and Pathology, Pasteur Institute, UMR1222 INSERM, 75015 Paris, France; §Laboratoire de Biochimie, Institut Chimie, Biologie, Innovation, UMR8231, ESPCI Paris, CNRS, Université Paris Sciences et Lettres, 75005 Paris, France; and ¶Sorbonne Université, Collège Doctoral, F-75005 Paris, France

ORCID: 0000-0001-9344-5110 (K.E.).

Received for publication January 31, 2020. Accepted for publication June 15, 2020.

This work was supported by funding from the The Branco Weiss Fellowship – Society in Science and funding from the European Research Council (ERC) under the European Union's Horizon 2020 Research and Innovation Program (Grant 80336) to K.E. This work has also received support from the Institut Pierre-Gilles de Gennes through Laboratoire d'Excellence, Investissements d'Avenir Programs ANR-10-IDEX-0001-02 PSL, ANR-10-EQPX-34, and ANR-10-LABX-31, and the ERC–Seventh Framework Program (ERC-2013-CoG 616050 to P.B.). C.C. acknowledges financial support from Consejo Nacional de Ciencia, Tecnología e Innovación Tecnológica, Peru.

Address correspondence and reprint requests to Prof. Klaus Eyer, ETH Zürich, Vladimir-Prelog-Weg 1-5/10, 8093 Zurich, Switzerland. E-mail address: klaus.eyer@pharma.ethz.ch

The online version of this article contains supplemental material.

Abbreviations used in this article: IgG-SC, IgG-secreting cell; TT, tetanus toxoid.

we followed the generation, evolution, and transfer of the IgG repertoire by using the snapshot analysis at more than 15 different days for one immunization protocol (8), achieving a good temporal resolution of the induced immune reaction. Although powerful and highly resolved, a thorough kinetic analysis using such an approach was time consuming, complex, and carried a high animal load. Because of these limitations, our method seemed unsuitable to characterize or optimize different immunization schemes.

However, within this original study, we observed a quick spike in the frequency and affinity of IgG-SCs early after recall with pure Ag (8). Because of the short time frame of their appearance and disappearance, we assumed that these cells were generated during the previous immunizations and were recalled to secrete IgG upon the injection of pure Ag. Therefore, we hypothesized that the recalled and reactivated IgG-SCs found in the spleen early after recall would be a good measure to characterize the preceding immunization protocol and give an integrative overview of the success rate of the generation, evaluation, and transfer of the immunization-induced IgG repertoire. Hence, in the study presented, we examined the impact of different immunization schemes on the quality and quantity of the generated, evolved, and transferred IgG repertoire by analyzing the IgG-SCs at 24 h after Ag recall. Secretion served, in this study, as a marker of activation. To be comparable to previous studies, we chose the established model Ag (tetanus toxoid [TT]) and a commonly used adjuvant. We first characterized the developed protocol and showed that 24 h after recall within the spleen was indeed the optimal time and place for the described analysis. Next, we introduced variations of immunization schemes to test the sensitivity of our measurement: variation of the primary immunization-boost interval and variation of the Ag dose should affect the quality of the IgG repertoire (7, 25–31). Lastly, the result of recalled cells were compared with cells present during the immunization itself to study the differences between recalled and initially generated secreted IgG repertoires. In this regard, the technology allowed extracting additional information when compared with ELISPOT (19, 20). In addition to frequencies with a defined threshold, affinities, and secretion rates were accessible with single-cell resolution allowing a quantitative analysis and description of the recalled, secreting Ab repertoire. This resolution is especially of interest early after recall, when only a few IgG-SCs have been activated and the secretion is too little to significantly alter the titer.

## Materials and Methods

A detailed protocol for the used *Materials and Methods* can be found in the literature (8, 32); the MATLAB code used for data analysis is available on the GitHub repository under https://github.com/LCMD-ESPCI/dropmap-analyzer.

### *Observation chamber assembly and droplet generator*

Microfluidic PDMS chip for droplet generation and observation chambers were fabricated as described elsewhere (8, 32).

### *Aqueous phase I: preparation of cells for droplet creation*

For droplet generation, cellular suspensions were centrifuged (300 × *g*, 5 min) and washed once in droplet media comprising RPMI 1640 without phenol red with supplemented 5% KnockOut Serum Replacement (both Thermo Fisher Scientific), 0.5% recombinant human serum albumin (A9986; Sigma-Aldrich), 25 mM HEPES (pH 7.4), 1% penicillin/streptomycin, and 0.1% Pluronic F-127 (all Thermo Fisher Scientific). The cells were resuspended in droplet media to achieve a λ (mean number of cells per droplet) of 0.2–0.4.

### *Aqueous phase II: beads and reagents*

Paramagnetic nanoparticles were prepared as described before (8, 32). For the sandwich immunoassay, CaptureSelect biotin anti-mouse IgGκ (L chain–specific) conjugate (Thermo Fisher Scientific) was used, and as a secondary, the non-IgG isotype–specific rabbit $F(ab')_2$ anti-mouse IgG Fc specific (Alexa647 labeled; Jackson ImmunoResearch) was added. Labeled TT (Statens Serum Institut, Copenhagen, Denmark) was labeled in house as a purified monomer with a degree of labeling of one fluorophore per TT monomer. Before use, the nanoparticles were resuspended thoroughly.

### *Data acquisition*

Droplets were generated as previously described (8, 32), and the emulsion was directly injected into the two-dimensional observation chamber. After chamber filling was complete, the chamber was gently closed and mounted onto an inverted fluorescence microscope (Ti Eclipse; Nikon). Two neodymium magnets (BZX082; K&J Magnetics) were placed on each side of the chamber during observation to hold the bead lines in place. Excitation light was provided by a LED source (SOLA Light Engine; Lumencor). Fluorescence for the specific channels were recorded using appropriate band pass filters (GFP and TRITC filter sets; Nikon, and Cy5 filter set; Semrock) and camera settings (Orca Flash 4; Hamamatsu) at room temperature (25°C) and ambient oxygen concentration. Images were acquired using a 10× objective (numerical aperture of 0.45). An array of 13 × 13 images were acquired for each experiment, every 7.5 min in all channels over 37.5 min (five measurements total).

### *Data analysis*

Data were analyzed using a custom-made MATLAB script (The MathWorks). The resulting raw data were exported to Excel (Microsoft), and sorted for droplets that showed an increase in anti-IgG relocation over time above a threshold. The selected droplets were controlled visually for the presence of a cell, and the absence of any fluorescent particles, relocation on cells (i.e., dead cells), or droplet movement. The so-selected droplets were analyzed to calculate secretion rates and dissociation constants calculated as described previously (8). The frequency of IgG-SCs was calculated using the number of cells present, and the number of selected droplets. The frequency of anti-Ag IgG-SCs was calculated using the number of cells present, and the number of cells found with a dissociation constant lower than 500 nM (limit of detection; see also Refs. 8 and 32). Frequencies are shown as percentages of IgG-SCs in cells analyzed from the B cell lineage.

### *Immunization of mice*

BALB-C mice were purchased from Janvier Labs (age 6–8 wk at start, female) and housed in the animal facilities of Institute Pasteur during experimentation. Mice were immunized with Ag (TT; Statens Serum Institut, or OVA; Invivogen) in adjuvant. Used adjuvants were either CFA (F5881; Sigma-Aldrich) or IFA (F5506; Sigma-Aldrich) mixed shortly before injection 1:1 with 0.9% (w/v) NaCl (Versylene; Fresenius). All immunizations were made i.p. Experiments using mice were validated by the CETEA ethics committee number 89 (Institute Pasteur, Paris, France) under no. 2013-0103, and by the French Ministry of Research under agreement no. 00513.02.

### *Extraction of IgG-SCs*

Spleens were harvested at the indicated time points of the immunization schedule. Spleen cell suspensions were recovered following disassociating using a 40-μm cell strainer. Cellular suspensions were pelleted at 300 × *g* for 5 min, and RBC lysis was performed for 1 min using BD Pharm Lyse (BD Biosciences). Cells were washed twice with MACS buffer and resuspended in 3 ml of MACS buffer. These cells were further processed according to the manufacturer's protocol using the Pan B Cell Isolation Kit II (Miltenyi) on a MultiMACS Cell24 Separator Plus (program depletion; Miltenyi). Purity of B cell lineage was usually above 90% (data not shown).

### *Titer measurements*

Standard anti-TT ELISA was performed on sera collected from all mice used in this manuscript, using 1 μg/ml TT (Reagent Proteins) for coating on MaxiSorp Nunc-Immuno plates (Thermo Fisher Scientific), 1% BSA (Sigma-Aldrich) for blocking, HRP-labeled anti-mouse Fc-specific Ab (Bethyl Laboratories) for detection, OPD (Sigma-Aldrich) for signal development, and 2 N $H_2SO_4$ for quenching. Absorbance was read thereafter at 492 nm using a spectrophotometer (Biophotometer; Eppendorf).

### *Statistical analysis*

We have performed each condition in triplicates (see Supplemental Table I for numbers of total and IgG-specific IgG-SCs per condition). The mean

values and their respective SD are shown on each figure and in the text if not mentioned otherwise. Median dissociation constants and secretion rates were calculated for each mouse, and the mean value over the triplicates is shown in the figures. Two-tailed Student *t* test was used to compare the differences in the values. Numbers of analyzed cells within each category are listed in Supplemental Table I. The original data used in this publication are made available in a curated data archive at ETH Zürich (https://www.research-collection.ethz.ch) under the DOI 330132.

## Results

### *DropMap methodology and extraction of parameters*

For each measurement described in the following figures, we used a recently developed and described microfluidic technology and workflow that we named DropMap (Fig. 1) (8, 32). Within DropMap, single–IgG-SCs are compartmentalized in tens of thousands of individual 50-pl droplets. Therefore, the secreted Ab repertoire can be analyzed with single-Ab resolution. To perform the measurement, we used a microfluidic observation chamber that forces these droplets to form a stable, stationary two-dimensional array. This array is monitored afterward by optical microscopy over time, allowing a kinetic analysis of secreted proteins. A fast and sensitive in droplet sandwich immunoassay that measures secreted murine IgG is employed within each droplet (Fig. 1B). Based on fluorescence relocation to magnetic nanoparticles, IgG secretion within a container results in an increase of fluorescence relocation onto the particles. The frequency of IgG-SCs was extracted by automatic counting of droplets with relocation above a certain threshold and are measured as a fraction of all present cells from the B cell lineage (see also *Materials and Methods* for purification strategy). Afterwards, secretion rates are extracted for each secreting cell by the use of a calibration curve and the relocation measurement over time of the anti-IgG signal. Additionally, relocation of fluorescently labeled Ag is measured; affinity can be assigned for Ab dissociation constants <500 nM. This affinity threshold is further used to calculate the frequency of TT-affine IgG-SCs that is displayed as the frequency within total cells.

### *Recall and activation of IgG-SCs after Ag injection is a rapid process*

First, we assessed the impact of the used recall method on the kinetics and appearance of the previously formed IgG-SCs in the spleen. Therefore, we immunized a series of mice with 10 μg of TT in CFA (day 0), 10 μg of TT in IFA (day 28), and challenged them with different recall conditions (day 56, Fig. 2A). Recalls were performed using 1 or 10 μg of TT in PBS, or 10 μg of TT in IFA; and mice were analyzed early (day 57 [i.e., within 24 h]) and late (day 60) after recall.

At day 56, a residual frequency of IgG-SCs of 0.58 ± 0.02% was present within the spleen (Fig. 2B). All assayed recall methods were able to show significantly higher frequencies at both days when compared with nonrecalled mice. Twenty-four hours afterward, the frequency of IgG-SCs within the spleen rises significantly in all conditions to 1.7 ± 0.1% ($p < 0.01$). As expected, this frequency continued to rise over the next 4 d (day 60) to 3.3–3.5% for recall with pure Ag, and up to 6.7 ± 0.2% ($p < 0.01$). Whereas the difference between IFA and Ag-only recalls was significantly different (due to the low half-life of the pure protein), the frequency of IgG-SCs for different doses of adjuvant-free recall methods was the same. However, all frequencies were significantly different from animals that were immunized but not

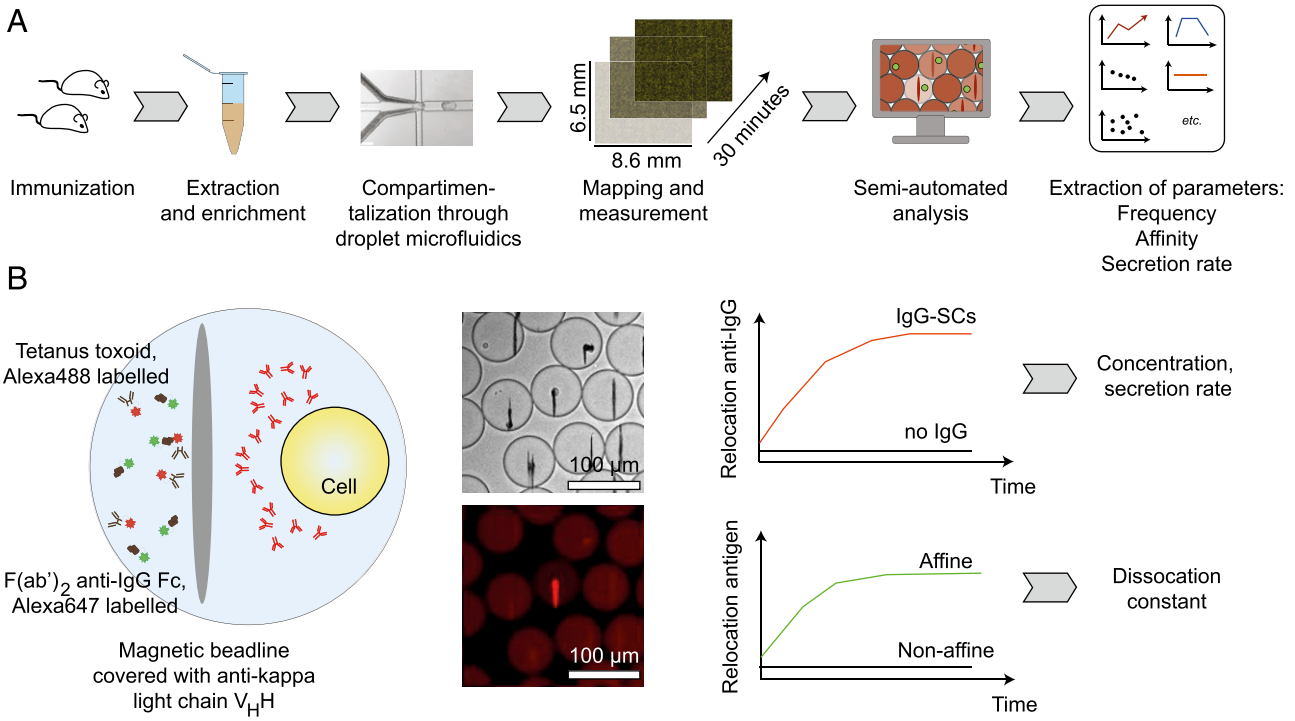


**FIGURE 1.** Overview of the DropMap workflow employed in this study. (**A**) BALB/C mice were immunized as described below. Splenocytes were extracted at indicated days, and the B cell linage was enriched. The individual cells are then compartmentalized in droplets, and the cellular IgG secretion is followed over time; parameters such as secretion rate, affinity, and frequencies were extracted on the individual cell basis. (**B**) Employed bioassay in the study are presented. Each droplet contained labeled Ag, labeled anti-IgG secondary, and around 1000 magnetic nanoparticles that were aligned to a beadline using a magnetic field. The images show droplets containing several cells, and one IgG-SCs in the droplet in the middle. Consequently, IgG secretion lead to fluorescence relocation on the beadline (center droplet). This relocation was extracted afterward and converted into concentration first (using calibration curves) and secretion rates thereafter. Similarly, relocation in the Ag channel was monitored, and with the information of the present concentration, the dissociation constant of the interaction was calculated.

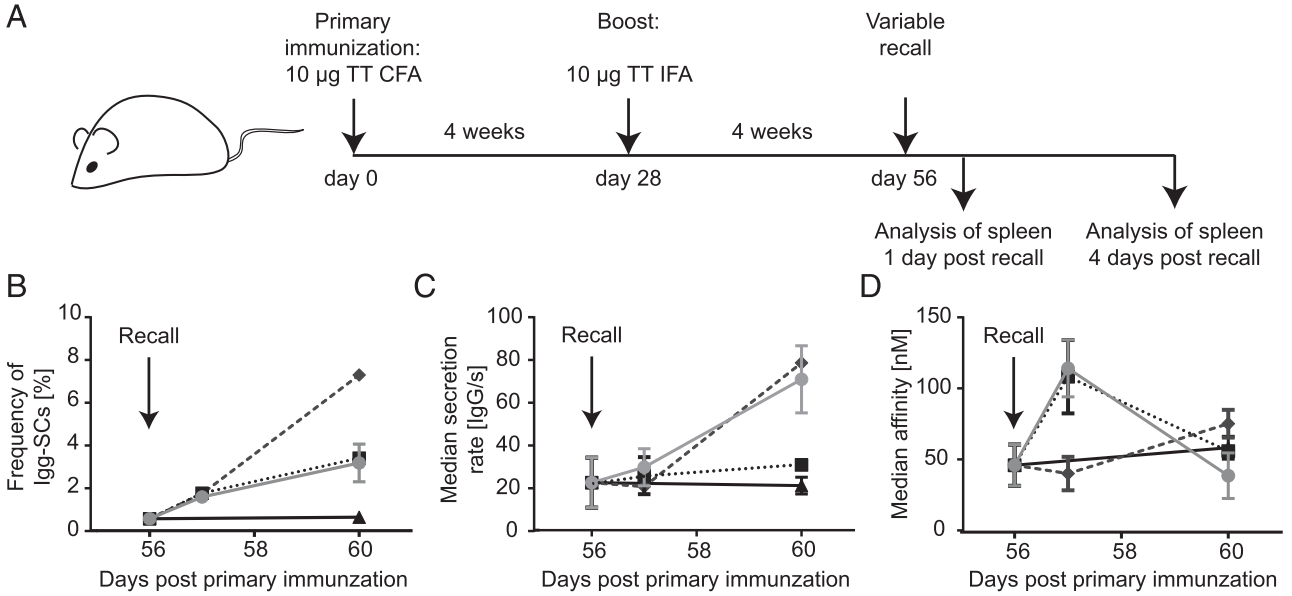


**FIGURE 2.** Recall and activation of IgG-SCs. (**A**) Deployed immunization schedule for the experiments to define the optimal recall method. In this study, primary immunization and boost were left constant (10 μg of TT in CFA and 10 μg of TT in IFA, respectively), and the recall method was varied: 1 μg of TT alone (circles, full line), 10 μg of TT alone (squares, pointed line), 10 μg of TT in IFA (diamond, dashed line) and no recall (triangle, full line). (**B**) Frequencies of IgG-SCs, (**C**) median secretion rate, and (**D**) median affinities at the day of the Ag recall (day 56), 24 h (day 57), and 4 d later (day 60). Frequencies are shown as percentages of IgG-SCs in cells analyzed from the B cell lineage. For all data points, $n = 1$ and $n = 3$ different mice for each condition, data are mean ± SD over the three mice.

recalled with Ag, where a constant frequency of IgG-SCs of around 0.60 ± 0.02% was present both at day 56 (day of the recall) and 60 (recall +4 d) for nonrecalled mice. At day 60, median secretion rates were also significantly different from nonrecalled mice ($p < 0.05$ for all conditions, Fig. 2C). In this study, the data were clustered by the amount of TT added to the recall and not specifically the method of recall (1 μg of TT as 72 ± 16 and 80 ± 2 IgG/s, and 31 ± 2 IgG/s for 10 μg of TT, all $p < 0.01$ when compared with recall-negative mice). In terms of median affinities, recalls with TT alone were found to reverse quickly toward the value found in nonrecalled mice (40 ± 16 nM for 1 μg of TT; 57 ± 4 nM for 10 μg of TT, 59 ± 8 nM for nonrecalled mice), whereas mice recalled using TT and IFA remained different (78 ± 10 nM for 10 μg of TT in IFA).

More surprisingly, the recall and reactivation of IgG-SCs was fast in all cases (<24 h) and the frequency of IgG-SCs increased significantly ~3-fold in recalled mice when compared with nonrecalled mice (day 57, 1.63 ± 0.18 and 0.58 ± 0.04%; mean ± SD, $p < 0.01$, Fig. 2B). Interestingly, the frequency of total IgG-SCs was nonsignificantly different for all three assayed recall methods early after said recall ($p > 0.28$) as well as the median secretion rates (Fig. 2C). In terms of median affinities of recalled cells, only recalls with pure Ag resulted in an increase in median dissociation constants (from 47 ± 15 nM at the day of recall to 115 ± 20 nM and 109 ± 25 nM, respectively, both $p < 0.05$, Fig. 2D; i.e., a loss of affinity). A recall with TT in IFA did not result in an efficient recall of low-affinity IgG-SCs (median affinity 41 ± 11 nM for IFA; nonsignificantly different from no recall). Therefore, free Ag was necessary to efficiently recall and activate the previously formed B cells to become IgG-SCs.

This early after the recall with pure Ag (24 h), a stimulation of naive cells to secrete IgG was unlikely because of the lag of a few days to induce an efficient germinal center response (33). Additionally, mice immunized with TT alone during immunizations did not show high frequencies of total IgG-SCs at this day (0.10 ± 0.01% compared with 0.05 ± 0.02% for naive mice, both $n = 3$), indicating that an injection of pure Ag was not able to induce such frequencies of IgG-SCs by itself. No significant decrease in the frequency of IgG-SCs in the bone marrow accompanied this increase in IgG-SCs within the spleens (data not shown), suggesting the absence of transfer of IgG-SCs from the bone marrow to the spleen. Given their secretion of IgG and various measured affinity for TT, we considered that the increase in total IgG-SCs 24 h after Ag recall must be related to the B cells formed during preceding immunizations that were efficiently recalled. In accordance with this hypothesis, recall with irrelevant Ag (primary immunization and boost with 1 μg of TT, recall with 5 μg of OVA) did not result in a significant increase in IgG-SCs within the first 24 h postrecall (0.30 ± 0.07% at day 56, 0.31 ± 0.14% at day 57, both $n = 3$, $p > 0.05$). To check for experimental variation within the chosen conditions, we repeated two experiments. Immunizations and analysis at day 57 was repeated for 1 and 10 μg of TT, respectively (Supplemental Table I). No significant differences were found in these repetitions, showing that the results were reproducible and the differences were due to the variation in immunization and boost.

The similarities early after recall, especially when free Ag was used, looked promising to continue with our hypothesis to use the recall analysis as a measure of the preceding immunization because an identical immunization protocol preceded the recall. We therefore opted to use a recall using 1 μg of TT in PBS alone and to analyze the IgG-SCs 24 h after recall within the spleen for all further presented data.

### *A shortening of primary immunizations skewed the repertoire significantly*

First, we decided to study the effect of shortened and prolonged prime-boost intervals on the quality and quantity of the recalled and activated IgG-SCs. Therefore, a subset of mice was immunized with 10 μg of TT in CFA/IFA, and the prime-boost interval was varied between 1 and 8 wk but followed by a constant boost-recall interval of 4 wk and a recall with pure Ag (Fig. 3A). In this study,

we found that the frequency of IgG-SCs 24 h after recall strongly correlated with the prime-boost interval in a time-dependent manner (Fig. 3B, effective time $ET_{50}$ = 2.88 ± 0.9 wk, $R^2$ = 0.94). The plateau observed around 4 wk was in agreement with germinal center kinetics (34), and was also consistent with our own experiments that showed the return to baseline in terms of Ab secretion and cellular frequency after around 3–4 wk using an identical immunization scheme (8). Median secretion rates were not significantly affected throughout this experimental series (Fig. 3C, slope −0.8 ± 0.2 IgG/s, $R^2$ = 0.88). Correlation was also observed for the frequency of Ag-specific IgG-SCs (Fig. 3D). Between 1 and 8 wk of prime-boost interval, the relation could be fitted linearly, showing an increase in the frequency of TT-affine IgG-SCs with prolonged primary immunizations (Δ% affine IgG-SC/week = 0.05 ± 0.01%/wk, $R^2$ = 0.96). Therefore, prolonged prime-boost interval resulted in increasing frequencies of TT-affine cells, as identified as cells secreting Abs displaying an affinity ($K_D$) <500 nM. However, median affinity best illustrated the impact of a rushed immunization protocol (Fig. 3E). Significantly lower affinities were found for shorter prime-boost intervals, even when measured after a constant boost period of 4 wk. The relation could be assumed linear between 1 and 8 wk (although the effects seemed to level off for even higher time intervals), and the median $K_D$ decreased of 8.3 ± 1.3 nM/wk of prime-boost interval ($R^2$ = 0.95).

### *Recall analysis reveals the influence of dose on the secreted IgG repertoire*

After visualizing the influence of prime-boost intervals, we wanted to measure the potential influence of the applied dose on the quality and quantity of recalled IgG-SCs, their affinity as well as secretion rates. Therefore, varying Ag doses were used in the immunization protocols, and the IgG-SCs were assayed 24 h after recall (Fig. 4A). An immunization with adjuvant alone (CFA/IFA only with 0 μg of TT during primary immunization and boost) resulted in the recall and activation of 0.95 ± 0.02% of IgG-SCs ($p < 0.01$ compared with recall-negative mice), although the recall was performed with pure TT in PBS (Fig. 4B). An increasing dose of used TT during primary immunization and boost was able to further raise the frequency of total IgG-SCs up to 1.70 ± 0.10% upon recall, doing so in a significant and dose-dependent manner (effective dose $ED_{50}$ = 0.22 ± 0.3 μg, $R^2$ = 0.86). Similar to the total frequency, the measured individual cellular secretion rates (Fig. 4C) displayed a dose-responsive trend toward higher secretion rates at higher TT doses ($ED_{50}$ = 1.4 ± 0.6 μg, $R^2$ = 0.70). In contrast, the interaction of the applied dose with the frequency of Ag-specific IgG-SCs followed a more complex, bell-shaped trend (Fig. 4D, Ag-specific IgG-SCs identified with dissociation constants [$K_D$] <500 nM) (8). The absolute frequency of TT-affine cells remained low from 0 μg of TT up to 0.3 μg of TT (0.07 ± 0.02% for 0 μg of TT) but showed a sharp and significant increase at higher doses (1–3 μg, both $p < 0.01$). However, the frequency of Ag-affine IgG-SCs decreased 2-fold thereafter when even higher amounts of Ag were used for immunization ($p < 0.05$). In contrast, at this Ag dose, the total number of IgG-SCs was still increasing (Fig. 4B). The impact of the only 3-fold increase in dose on the extracted frequency of TT-affine IgG-SCs was surprising. Therefore, the experiment with the 10-μg TT dose was repeated three times independently (different batch of mice, different cages, and different times), and the decrease in the frequency of Ag-affine IgG-SCs was confirmed (data not shown). Simultaneously, median affinity ($K_D$) itself also showed a more complex interaction with dose (Fig. 4E). As expected, the median $K_D$ extracted from the IgG-SCs immunized without any Ag (CFA/IFA alone) was nonsignificantly different from to the median $K_D$ found in naive mice (155 ± 6 nM, $n$ = 3; and 161 ± 17 nM, $n$ = 3). When TT was added to the immunizations, the median $K_D$ showed a rapid, clear, and significant trend toward high-affinity anti-TT Abs with an optimum dose of 1 μg of TT (57 ± 15 nM, $n$ = 3). However, higher doses of TT (3–10 μg) resulted in a significant loss in affinity (median $K_D$ 130

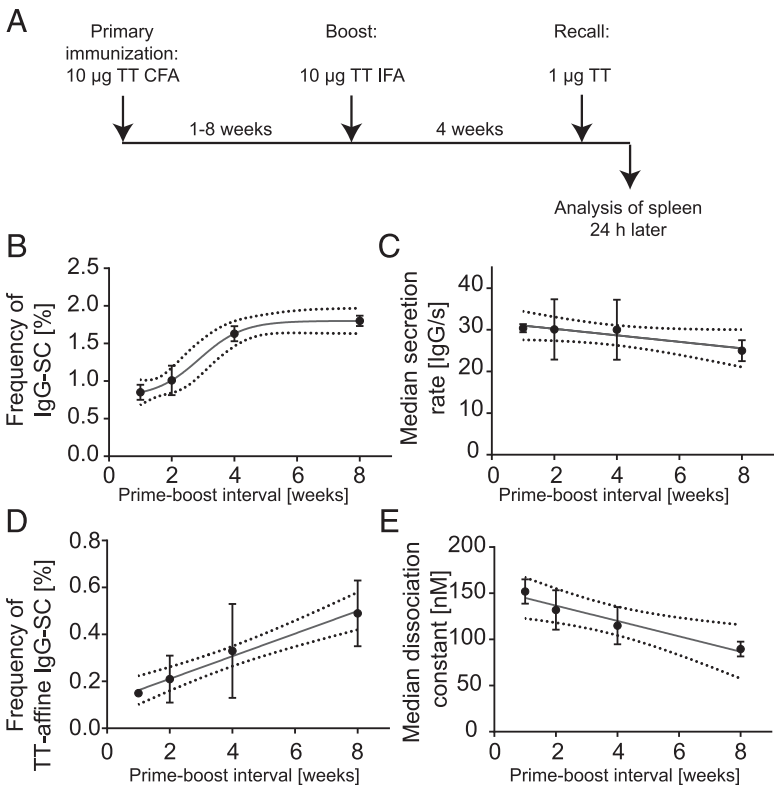


**FIGURE 3.** Correlation with timing of immunization. (**A**) Mouse immunization scheme for the data presented in this figure. (**B**) Frequency of IgG-SCs as a measure of different prime-boost intervals. (**C**) Median secretion rate in IgG/s as a function of different prime-boost intervals. (**D**) Frequency of TT-affine IgG-SCs ($K_D$ < 500 nM) as a measure of different prime-boost intervals. (**E**) Median dissociation constant extracted for TT-affine cells as measure of different prime-boost intervals. For all data points, $n$ = 1 and $n$ = 3 different mice for each condition; data are mean ± SD over the three mice. The dotted lines represents the confidence interval of the fits.

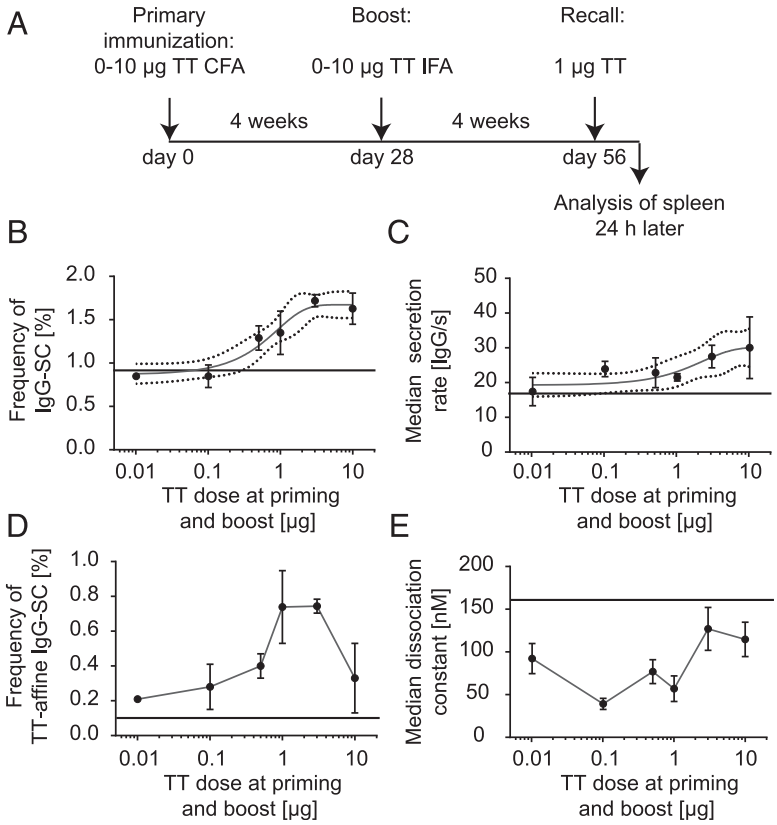


**FIGURE 4.** Affinity maturation after immunization using CFA/IFA as adjuvants and various doses of TT as Ag. (**A**) Mouse immunization scheme for the data presented in this figure. (**B**–**E**) Summary of the CFA/IFA immunizations. (B) Frequency of IgG-SCs as a measure of the used dose of TT. (C) Median secretion rate in IgG/s as a measure of the dose used to immunize. (D) Frequency of TT-affine IgG-SCs ($K_D < 500$ nM) as a measure of the dose used to immunize. (E) Median dissociation constant extracted for TT-affine cells. For all data points, $n = 1$ and $n = 3$ different mice for each condition; data are mean ± SD over the three mice. The solid horizontal line represents the value measured for mice immunized with adjuvant only, and the dotted lines in (B) and (C) the confidence interval of the fits.

± 10 nM). This decrease in affinity was sharp and narrow; and the extent of this decrease was highly reproducible ($N_{replicates} = 3$, $n_{mice} = 3$ for each replicate for 10 μg of TT). The experiments described in Figs. 3 and 4 confirmed the hypothesis that the recalled IgG repertoire was shaped by the preceding immunization, as defined by the interaction of dose and prime-boost intervals. In parallel, we also assessed the titers in all the immunized mice. As expected, the titer was not a suitable measure to capture and dissect these fast and highly complex interactions of dose with frequency and affinity. Instead, titers simply increased with added dose of Ag (Supplemental Fig. 1).

*Recall analysis correlated with observations during the preceding immunization, but also showed differences in the transfer success of TT-specific cells*

Our analysis of the repertoire 24 h after recall was able to show significant differences in the success rates to be recall available for IgG-SCs. These differences were induced by variations of dose and adjuvant. However, it was not clear how the secreted IgG repertoire measured after recall correlated with the repertoire present during immunization itself. To therefore demonstrate similarities and differences in quality and quantity, we assayed a cohort of mice 32 d after primary immunization (i.e., 4 d after boost) and correlated this data with the results that we observed at day 57 (i.e., 24 h after Ag recall; Fig. 5).

First, we found a strong correlation between the frequency of IgG-SCs after recall and during immunization (Fig. 5B, $R^2 = 0.93$). However, this correlation was not of linear nature and leveled at 1.77 ± 0.11% IgG-SCs after recall. Although higher frequencies of total IgG-SCs were generated during boost, the frequency of IgG-SCs available for recall and activation from previous immunizations was limited. More surprisingly, median secretion rates after recall correlated with those found during boost (Fig. 5C). A linear trend between the two analysis days was found (slope 0.50 ± 0.02, $R^2 = 0.99$) that further correlated also with the dose of TT. As for TT-affine IgG-SCs, a perfect correlation of the frequencies of Ag-specific IgGs was found up to a dose of 1 μg (overlay of the two lines in Fig. 5D). Higher TT doses were not able to translate their initial high frequencies into the recalled IgG-SCs (i.e., the points are below the black line), explaining the observed differences in the titer measurements. Although more TT-specific cells were induced during immunization, at higher doses (3–10 μg) these initial high frequencies did not translate into high frequencies after recall. Additionally, the extracted median $K_D$ values, also showed a more complex interaction between the 2 d (Fig. 5E). When comparing median $K_D$ values at day 32 (day 4 after boost) with median $K_D$ values 24 h after recall, a good correlation was only found up to 1 μg of TT dose. Higher Ag doses, such as 3 and 10 μg of TT, deviated strongly from this trend. When 3 μg of TT was used for immunization, the median $K_D$ value of the recalled TT-affine IgG-SCs was found to be lower than at day 32 during boost, showing that at this Ag dose the TT-affine IgG-SCs were not efficiently transferred to respond to recall challenge (as also visible in the lower frequency). A higher TT dose of 10 μg of TT was not able to generate significant amounts of high-affinity TT-affine IgG-SCs, most probably because of the absence of efficient selection and affinity maturation at this dose.

## Discussion

In this study, we used a novel, to our knowledge, ex vivo analysis method (DropMap) (8) in combination with a rather unusual analysis point (24 h after recall) to quantitatively describe the quality of the IgG repertoire that is able to respond to re-exposure to Ag. This recalled and activated secreted IgG repertoire will also be part of the IgG repertoire that is available in vivo after re-exposure with Ag due to infection or challenge. Because of the generation of high-resolution snapshots, the protocol allowed for a quantitative study of the rapid changes after recall and activation

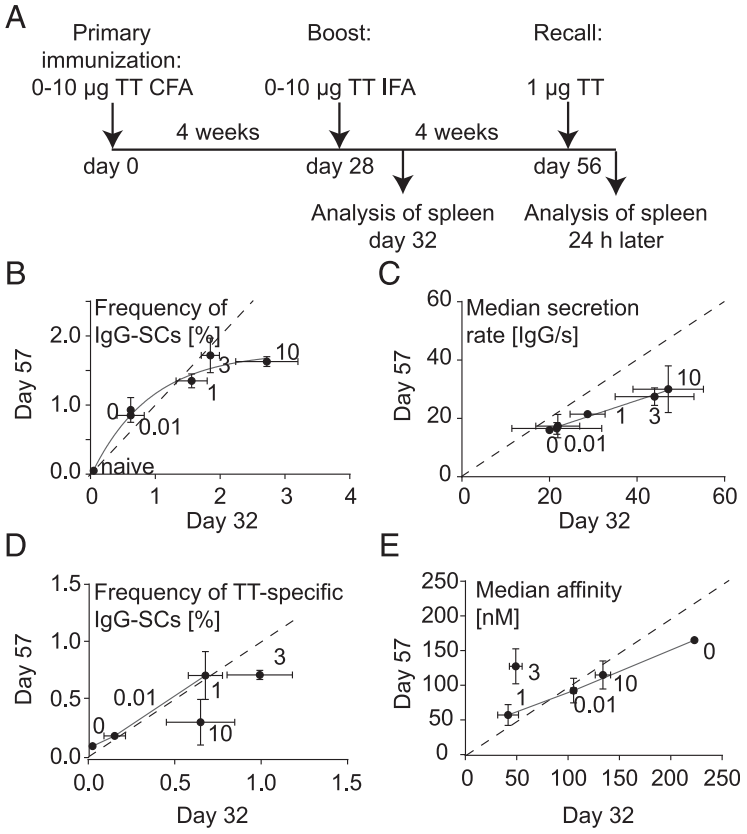


**FIGURE 5.** Correlation of recall immunization with boost. (**A**) Mouse immunization scheme for the data presented in this figure. (**B**) Correlation found for the total frequency of IgG-SCs between day 32 (day 4 after boost) and day 57 (day 1 after recall). The interaction seems to level off. (**C**) Observed correlation for extracted median secretion rates. (**D**) Dependence of TT-affine IgG-SCs and (**E**) their median affinity for TT. Dashed black lines represent a correlation of 1, whereas solid lines represent the fitted correlation. Each point represents a different Ag dose of TT. For all data points, $n = 1$ and $n = 3$ different mice for each condition; data are mean ± SD over the three mice.

of previously formed B cells and was able to resolve significant differences in the previously employed immunizations. First, we were able to show that this approach was able to capture the fast recall and activation to secrete IgG (3- to 4-fold increase in total IgG-SCs after 24 h). This effect was not caused by an unspecific effect due to protein administration. Indeed, a recall with irrelevant Ag (OVA) did not result in a significant increase in IgG-SCs. Interestingly, only a fraction of the recalled IgG-SCs were indeed Ag-specific. When TT was used for primary immunization and boost, only 33 ± 9% of IgG-SCs were found to have a dissociation constant <500 nM, in this study identified as being affine for TT, whereas the rest of the cells either have a nonmeasurable affinity for TT or are activated through bystander effects. Furthermore, an analysis at this time point was also not contaminated significantly with a new, naive response that was detectable 4 d after recall. Only because of the resolution and sensitivity of the employed technology were we able to use this early day for the characterization of the impact of various immunization protocols thereafter. We could further show that the secreted repertoire measured 24 h after recall correlated nicely and significantly with the preceding immunization (Figs. 3, 4); together with a variety of control experiments, this finding suggested that the IgG-SCs measured after recall indeed stemmed from previous immunizations. This recalled IgG repertoire shared features with the secreted repertoire that was present during the preceding immunizations but also showed significant differences. The intention of most immunization is to generate high-affinity IgG-SCs that are present at a certain frequency. Interestingly, those two parameters showed the most complex behavior within recalled IgG-SCs (Figs. 3, 4) and also when we compared the recalled and activated part of the IgG repertoire with the secreted repertoire present during the immunization itself (Fig. 5). Specific doses of TT showed significantly higher frequencies of TT-specific IgG-SCs and lower median $K_D$ during the preceding immunization, but these values never translated to the recalled IgG-SCs. In this study, the absence of efficient affinity maturation as well as selection might interfere with an efficient increase of TT-affine cells to the moment when memory cells are generated within the germinal center (35–39), therefore explaining the lack of correlation with the titer measurements that were not able to either capture nor resolve these complex interactions. As expected, a compression of the period of immunization (Fig. 4) resulted in a smaller and less affine repertoire. Interestingly, the impact of the compressed prime-boost interval was not compensated for during the repeated constant immunization period, displaying a variation of the original sin problem (40, 41). As shown by these examples, and in contrast to titer or measurements during immunization, the study of the translated and reactivated part of the IgG repertoire might represent a more direct and functional measure of the efficiency and quality of the immunization-induced IgG repertoire of the vaccination.

Limitations of the approach are possible biases due to varying recall efficiencies and kinetics due to differences stemming from various induced immune reactions. Various Ags, additives, and adjuvants might change the kinetics of recall and, therefore, also the results solely because of the change in kinetics. Even within these experiments presented in this study, it is safe to assume that not all cells will be recalled and activated within the first 24 h and, therefore, only a part of the generated response was measured. Over time, additional cells will be added the secreted IgG repertoire, although in the presence of a naive response due to the injection of Ag. Moreover, secreting cells may still always represent a bias sampling of all nonnaive B cells. Nevertheless, the strong correlations found within this project suggest a strong dependence of the measurement of recall-activated IgG-SCs with the preceding immunizations, but further studies are needed to quantify similarities and differences. Additionally, the transfer of the developed approach to human immunization protocols is not easily feasible

because of the inaccessibility of secondary lymphoid tissues in most clinical studies and allotted ethical protocols.

Nonetheless, these data sets further highlight the power of highly resolved and quantitative single-cell analysis approaches such as DropMap, and their use in the study and quantification of immunization and vaccination schemes. This study showed the feasibility of characterizing the integrity of immunization-induced processes with a single time point measurement 24 h after recall. This simple measurement may be used as a surrogate test to optimize new vaccination schemes. Additionally, this study also revealed and opened a variety of scientific questions to explore such as the influence of recall/challenge on the recalled repertoire and the mechanistic reasons for the differences observed in Fig. 5. Exemplarily, the interaction between dose and median affinity was nontrivial, showing a clear optimum. Recent vaccination studies in humans also showed similar nontrivial relationship between dosage and the Ab response (42–45), showing the need to analyze the complex humoral reaction with single-Ab resolution. In this study, an analytical pathway as the one presented might help to shed light into the underlying mechanisms. This quantitative data will also serve as a great basis for the modeling of the immune reaction and the resulting secreted IgG repertoire (46).

## Disclosures

The authors have no financial conflicts of interest.

## References


1. Asensio, M. A., Y. W. Lim, N. Wayham, K. Stadtmiller, R. C. Edgar, J. Leong, R. Leong, R. A. Mizrahi, M. S. Adams, J. F. Simons, et al. 2019. Antibody repertoire analysis of mouse immunization protocols using microfluidics and molecular genomics. *MAbs* 11: 870–883.
2. Chung, A. W., M. P. Kumar, K. B. Arnold, W. H. Yu, M. K. Schoen, L. J. Dunphy, T. J. Suscovich, N. Frahm, C. Linde, A. E. Mahan, et al. 2015. Dissecting polyclonal vaccine-induced humoral immunity against HIV using systems serology. *Cell* 163: 988–998.
3. Lavinder, J. J., Y. Wine, C. Giesecke, G. C. Ippolito, A. P. Horton, O. I. Lungu, K. H. Hoi, B. J. DeKosky, E. M. Murrin, M. M. Wirth, et al. 2014. Identification and characterization of the constituent human serum antibodies elicited by vaccination. *Proc. Natl. Acad. Sci. USA* 111: 2259–2264.
4. Coffman, R. L., A. Sher, and R. A. Seder. 2010. Vaccine adjuvants: putting innate immunity to work. *Immunity* 33: 492–503.
5. Cribbs, D. H., A. Ghochikyan, V. Vasilevko, M. Tran, I. Petrushina, N. Sadzikava, D. Babikyan, P. Kesslak, T. Kieber-Emmons, C. W. Cotman, and M. G. Agadjanyan. 2003. Adjuvant-dependent modulation of Th1 and Th2 responses to immunization with beta-amyloid. *Int. Immunol.* 15: 505–514.
6. Pulendran, B., and R. Ahmed. 2011. Immunological mechanisms of vaccination. *Nat. Immunol.* 12: 509–517.
7. Eisen, H. N. 2014. Affinity enhancement of antibodies: how low-affinity antibodies produced early in immune responses are followed by high-affinity antibodies later and in memory B-cell responses. *Cancer Immunol. Res.* 2: 381–392.
8. Eyer, K., R. C. L. Doineau, C. E. Castrillon, L. Briseño-Roa, V. Menrath, G. Mottet, P. England, A. Godina, E. Brient-Litzler, C. Nizak, et al. 2017. Single-cell deep phenotyping of IgG-secreting cells for high-resolution immune monitoring. *Nat. Biotechnol.* 35: 977–982.
9. Radbruch, A., G. Muehlinghaus, E. O. Luger, A. Inamine, K. G. Smith, T. Dörner, and F. Hiepe. 2006. Competence and competition: the challenge of becoming a long-lived plasma cell. *Nat. Rev. Immunol.* 6: 741–750.
10. Shulman, Z., A. D. Gitlin, J. S. Weinstein, B. Lainez, E. Esplugues, R. A. Flavell, J. E. Craft, and M. C. Nussenzweig. 2014. Dynamic signaling by T follicular helper cells during germinal center B cell selection. *Science* 345: 1058–1062.
11. D'Angio, C. T., C. P. Wyman, R. S. Misra, J. L. Halliley, H. Wang, J. E. Hunn, C. M. Fallone, and F. E. Lee. 2017. Plasma cell and serum antibody responses to influenza vaccine in preterm and full-term infants. *Vaccine* 35: 5163–5171.
12. Wine, Y., A. P. Horton, G. C. Ippolito, and G. Georgiou. 2015. Serology in the 21st century: the molecular-level analysis of the serum antibody repertoire. *Curr. Opin. Immunol.* 35: 89–97.
13. Szczawinska-Poplonyk, A., A. Breborowicz, H. Samara, L. Ossowska, and G. Dworacki. 2015. Impaired antigen-specific immune response to vaccines in children with antibody production defects. *Clin. Vaccine Immunol.* 22: 875–882.
14. Wine, Y., D. R. Boutz, J. J. Lavinder, A. E. Miklos, R. A. Hughes, K. H. Hoi, S. T. Jung, A. P. Horton, E. M. Murrin, A. D. Ellington, et al. 2013. Molecular deconvolution of the monoclonal antibodies that comprise the polyclonal serum response. *Proc. Natl. Acad. Sci. USA* 110: 2993–2998.
15. Deng, R., D. Bumbaca, C. V. Pastuskovas, C. A. Boswell, D. West, K. J. Cowan, H. Chiu, J. McBride, C. Johnson, Y. Xin, et al. 2016. Preclinical pharmacokinetics, pharmacodynamics, tissue distribution, and tumor penetration of anti-PD-L1 monoclonal antibody, an immune checkpoint inhibitor. *MAbs* 8: 593–603.
16. Vieira, P., and K. Rajewsky. 1988. The half-lives of serum immunoglobulins in adult mice. *Eur. J. Immunol.* 18: 313–316.
17. Nossal, G. J., and O. Makela. 1962. Elaboration of antibodies by single cells. *Annu. Rev. Microbiol.* 16: 53–74.
18. Leyendeckers, H., M. Odendahl, A. Löhndorf, J. Irsch, M. Spangfort, S. Miltenyi, N. Hunzelmann, M. Assenmacher, A. Radbruch, and J. Schmitz. 1999. Correlation analysis between frequencies of circulating antigen-specific IgG-bearing memory B cells and serum titers of antigen-specific IgG. *Eur. J. Immunol.* 29: 1406–1417.
19. Czerkinsky, C. C., L. A. Nilsson, H. Nygren, O. Ouchterlony, and A. Tarkowski. 1983. A solid-phase enzyme-linked immunospot (ELISPOT) assay for enumeration of specific antibody-secreting cells. *J. Immunol. Methods* 65: 109–121.
20. Saletti, G., N. Çuburu, J. S. Yang, A. Dey, and C. Czerkinsky. 2013. Enzyme-linked immunospot assays for direct ex vivo measurement of vaccine-induced human humoral immune responses in blood. *Nat. Protoc.* 8: 1073–1087.
21. Busse, C. E., I. Czogiel, P. Braun, P. F. Arndt, and H. Wardemann. 2014. Single-cell based high-throughput sequencing of full-length immunoglobulin heavy and light chain genes. *Eur. J. Immunol.* 44: 597–603.
22. DeKosky, B. J., G. C. Ippolito, R. P. Deschner, J. J. Lavinder, Y. Wine, B. M. Rawlings, N. Varadarajan, C. Giesecke, T. Dörner, S. F. Andrews, et al. 2013. High-throughput sequencing of the paired human immunoglobulin heavy and light chain repertoire. *Nat. Biotechnol.* 31: 166–169.
23. McDaniel, J. R., B. J. DeKosky, H. Tanno, A. D. Ellington, and G. Georgiou. 2016. Ultra-high-throughput sequencing of the immune receptor repertoire from millions of lymphocytes. *Nat. Protoc.* 11: 429–442.
24. Shembekar, N., H. Hu, D. Eustace, and C. A. Merten. 2018. Single-cell droplet microfluidic screening for antibodies specifically binding to target cells. *Cell Rep.* 22: 2206–2215.
25. Allen, C. D., T. Okada, and J. G. Cyster. 2007. Germinal-center organization and cellular dynamics. *Immunity* 27: 190–202.
26. Gitlin, A. D., Z. Shulman, and M. C. Nussenzweig. 2014. Clonal selection in the germinal centre by regulated proliferation and hypermutation. *Nature* 509: 637–640.
27. Oropallo, M. A., and A. Cerutti. 2014. Germinal center reaction: antigen affinity and presentation explain it all. *Trends Immunol.* 35: 287–289.
28. Tam, H. H., M. B. Melo, M. Kang, J. M. Pelet, V. M. Ruda, M. H. Foley, J. K. Hu, S. Kumari, J. Crampton, A. D. Baldeon, et al. 2016. Sustained antigen availability during germinal center initiation enhances antibody responses to vaccination. *Proc. Natl. Acad. Sci. USA* 113: E6639–E6648.
29. Tas, J. M. J., L. Mesin, G. Pasqual, S. Targ, J. T. Jacobsen, Y. M. Mano, C. S. Chen, J. C. Weill, C. A. Reynaud, E. P. Browne, et al. 2016. Visualizing antibody affinity maturation in germinal centers. *Science* 351: 1048–1054.
30. Turner, J. S., F. Ke, and I. L. Grigorova. 2018. B cell receptor crosslinking augments germinal center B cell selection when T cell help is limiting. *Cell Rep.* 25: 1395–1403.e4.
31. Victora, G. D., and P. C. Wilson. 2015. Germinal center selection and the antibody response to influenza. *Cell* 163: 545–548.
32. Bounab, Y., K. Eyer, S. Dixneuf, M. Rybczynska, C. Chauvel, M. Mistretta, T. Tran, N. Aymerich, G. Chenon, J. F. Llitjos, et al. Dynamic single-cell phenotyping of immune cells. *Nat. Protoc.* In press.
33. Gitlin, A. D., L. von Boehmer, A. Gazumyan, Z. Shulman, T. Y. Oliveira, and M. C. Nussenzweig. 2016. Independent roles of switching and hypermutation in the development and persistence of B lymphocyte memory. *Immunity* 44: 769–781.
34. Mesin, L., J. Ersching, and G. D. Victora. 2016. Germinal center B cell dynamics. *Immunity* 45: 471–482.
35. Kräutler, N. J., D. Suan, D. Butt, K. Bourne, J. R. Hermes, T. D. Chan, C. Sundling, W. Kaplan, P. Schofield, J. Jackson, et al. 2017. Differentiation of germinal center B cells into plasma cells is initiated by high-affinity antigen and completed by Tfh cells. *J. Exp. Med.* 214: 1259–1267.
36. O'Connor, B. P., L. A. Vogel, W. Zhang, W. Loo, D. Shnider, E. F. Lind, M. Ratliff, R. J. Noelle, and L. D. Erickson. 2006. Imprinting the fate of antigen-reactive B cells through the affinity of the B cell receptor. *J. Immunol.* 177: 7723–7732.
37. Phan, T. G., D. Paus, T. D. Chan, M. L. Turner, S. L. Nutt, A. Basten, and R. Brink. 2006. High affinity germinal center B cells are actively selected into the plasma cell compartment. *J. Exp. Med.* 203: 2419–2424.
38. Smith, K. G., A. Light, G. J. Nossal, and D. M. Tarlinton. 1997. The extent of affinity maturation differs between the memory and antibody-forming cell compartments in the primary immune response. *EMBO J.* 16: 2996–3006.
39. Weisel, F. J., G. V. Zuccarino-Catania, M. Chikina, and M. J. Shlomchik. 2016. A temporal switch in the germinal center determines differential output of memory B and plasma cells. *Immunity* 44: 116–130.
40. Monto, A. S., R. E. Malosh, J. G. Petrie, and E. T. Martin. 2017. The doctrine of original antigenic sin: separating good from evil. *J. Infect. Dis.* 215: 1782–1788.
41. Vatti, A., D. M. Monsalve, Y. Pacheco, C. Chang, J. M. Anaya, and M. E. Gershwin. 2017. Original antigenic sin: a comprehensive review. *J. Autoimmun.* 83: 12–21.
42. Aagaard, C., T. Hoang, J. Dietrich, P. J. Cardona, A. Izzo, G. Dolganov, G. K. Schoolnik, J. P. Cassidy, R. Billeskov, and P. Andersen. 2011. A multistage tuberculosis vaccine that confers efficient protection before and after exposure. *Nat. Med.* 17: 189–194.
43. Aagaard, C., T. T. Hoang, A. Izzo, R. Billeskov, J. Troudt, K. Arnett, A. Keyser, T. Elvang, P. Andersen, and J. Dietrich. 2009. Protection and

polyfunctional T cells induced by Ag85B-TB10.4/IC31 against Mycobacterium tuberculosis is highly dependent on the antigen dose. *PLoS One* 4: e5930.

44. Luabeya, A. K. K., B. M. N. Kagina, M. D. Tameris, H. Geldenhuys, S. T. Hoff, Z. Shi, I. Kromann, M. Hatherill, H. Mahomed, W. A. Hanekom, et al; H56-032 Trial Study Group. 2015. First-in-human trial of the post-exposure tuberculosis vaccine H56:IC31 in Mycobacterium tuberculosis infected and non-infected healthy adults. *Vaccine* 33: 4130–4140.
45. Rhodes, S. J., A. Zelmer, G. M. Knight, S. A. Prabowo, L. Stockdale, T. G. Evans, T. Lindenstrøm, R. G. White, and H. Fletcher. 2016. The TB vaccine H56+IC31 dose-response curve is peaked not saturating: data generation for new mathematical modelling methods to inform vaccine dose decisions. *Vaccine* 34: 6285–6291.
46. Molari, M., K. Eyer, J. Baudry, S. Cocco, and R. Monasson. 2020. Quantitative modeling of the effect of antigen dosage on B-cell affinity distributions in maturating germinal centers. *eLife* 9: e55678.